SAND2012-1598 C
SAND2012-1598C

Simple Shock Physics Models—Initial Studies for Real Applied Problems

or

A "Green" Talk—Recycling Old (but useful) Tools

Jeff Lawrence, Retired
Sandia National Laboratories
Albuquerque, New Mexico

With input from:
Mike Furnish, Sandia National Laboratories
John Remo, Harvard University

Sandia National Laboratories is a multi-program laboratory managed and operated by Sandia Corporation, a wholly owned subsidiary of Lockheed Martin Corporation, for the U.S. Department of Energy's National Nuclear Security Administration under contract DE-AC04-94AL85000.

A brief summary of impact and penetration for missile-defense applications . . .

Impact and shock physics are disciplines required to predict the effects and consequences of various types of kinetic-energy-based missile-defense engagement scenarios.

Generic processes for missile-defense engagements

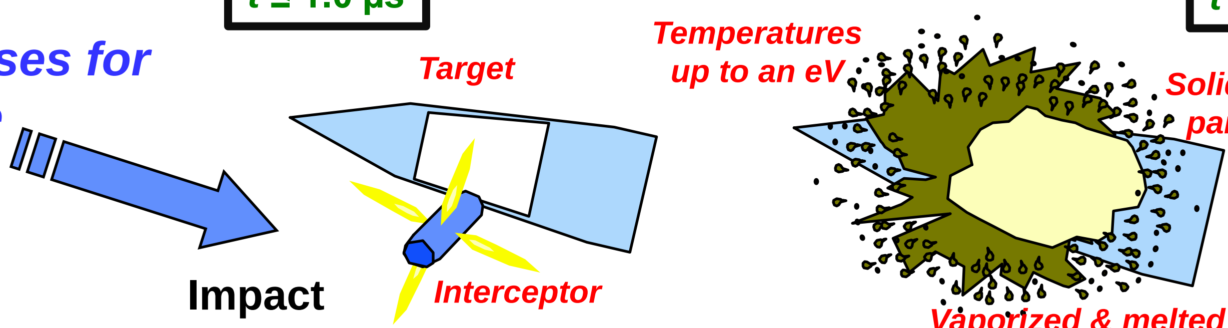

Impact flash

Shock-wave & material response

Late-time thermal radiation

Penetration & fragmentation

External debris

Internal debris

Structural response

Specific approaches that are needed include laboratory-scale experiments, numerical modeling (1-D & multi-D), and analytic and scaling-law analyses.

Sandia National Laboratories

Targets are *thick* or *thin*; projectiles are "*chunky*" ($L/D \approx 1$) or *long-rods* ($L/D >> 1$).

- Targets are *thick* (non-penetrating) or *thin* (penetrating) based roughly on the ratio of the main projectile dimension to the target thickness.
  - For *thick* targets, crater depth (or volume) is the main impact metric.
  - For *thin* targets, V_{50} and the characteristics of the fragment or debris clouds are of more importance.
  - *Layered* targets can usually be treated as combinations of *thick* and *thin* constituents.
  - Most effects for $L/D << 1$ projectiles can usually be treated with $L/D \approx 1$ modeling.
  - Detonation of energetic materials (*e.g.*, high explosives) contained in targets can be treated with $p^2\Delta\tau$ or similar criteria.
- Basic penetration by either $L/D = 1$ or $L/D >> 1$ projectiles can be analyzed with: 1) simple but different scaling laws; 2) detailed analytic models; and 3) multi-dimensional hydrocodes.
- Variations can include projectiles incorporating energetic materials.
  - High explosives have an energy content of ~1000 cal/g, which is the same as the specific kinetic energy of a projectile with a velocity of ~3 km/s.
  - Although valuable for lower velocities, engagements at greater than 3 km/s by even a modest factor (recall that $KE \propto V^2$), offer little advantage for energetic-material projectiles.

Sandia National Laboratories

Target penetration depth can depend strongly on projectile shape.

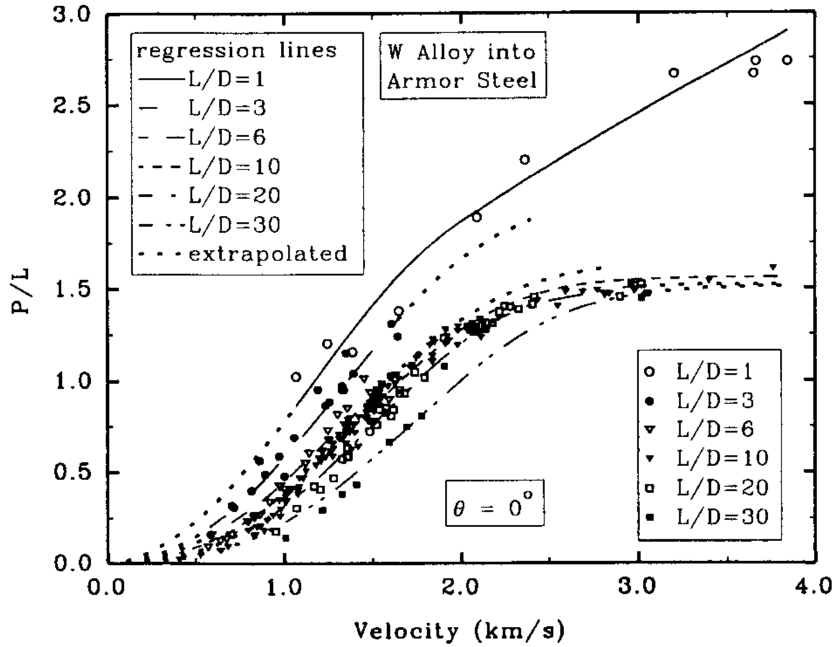

- **Penetration *efficiency* (*P/L*) is actually better for "chunky" (*L/D* ≈ 1) projectiles than for long rods (*L/D* large).**
- **Limiting penetration, *P*, for long rods is:**
  - > $P/L = (\rho_{projectile}/\rho_{target})^{1/2}$, [$V_{projectile}$ > few km/s];
  - > Holds well for pitch and yaw up to ~15°;
  - > Oblique targets can introduce rod rotation;
  - > Results hold for shaped-charge jets.
- **While for chunky projectiles:**
  - > $P \propto (\rho_{projectile}/\rho_{target})^{1/3} (V_{projectile})^{2/3}$;
  - > Similar scaling holds for explosively-formed projectiles (EFPs).

Low-density materials are preferred for targets because low total mass is always desired. Target mass goes linearly with density, while improved penetration resistance goes only as $\rho^{1/2}$, at best. High projectile density always improves penetration. Thus projectiles are often high-density, e.g., depleted uranium (DU) or tungsten (W). The scaling laws show why "segmented" rods—made from spaced "chunky" projectiles—improve performance.

– Data from Anderson (1992).

The impact-velocity "cliff" has been investigated explicitly only rarely.

Structural failure for stand-off shields

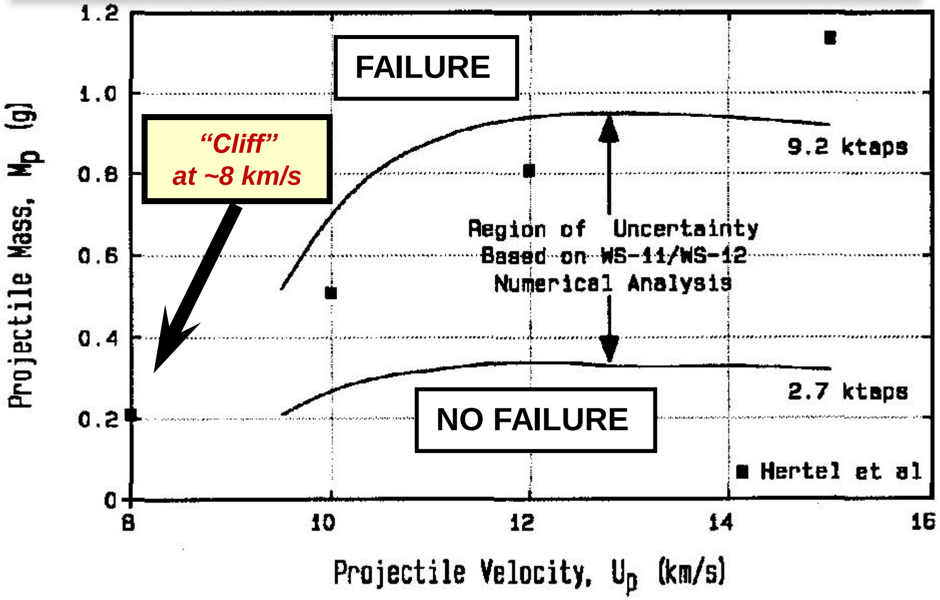

For plotted failure data:

- ***Curves are from analytic theory, based on experiments;***
- ***Points are from multi-D numerical calculations;***
- ***Configuration is Al projectile impacting an Al stand-off shield w/ Al substructure.***

- **The "cliff" is defined in terms of the velocity above which the impact products are dominated by material decomposition; below the cliff, melting and vaporization play a much smaller role.**
- **Note that above the cliff, the results for structural failure go in a counter-intuitive direction.**
- **Traditional experimental gas-gun techniques are generally limited to conditions below the cliff.**
- **Experimental trends below the velocity cliff *cannot be extrapolated* to regimes above the cliff.**
- **There are only two approaches to obtain data "above the cliff":**
  - > **Conduct experiments at higher velocities;**
  - > **Shift the cliff to lower velocities.**

– Data & model from Lawrence (1992a).

Sandia National Laboratories

Experiments above the cliff are difficult; surrogate materials may be the easiest approach.

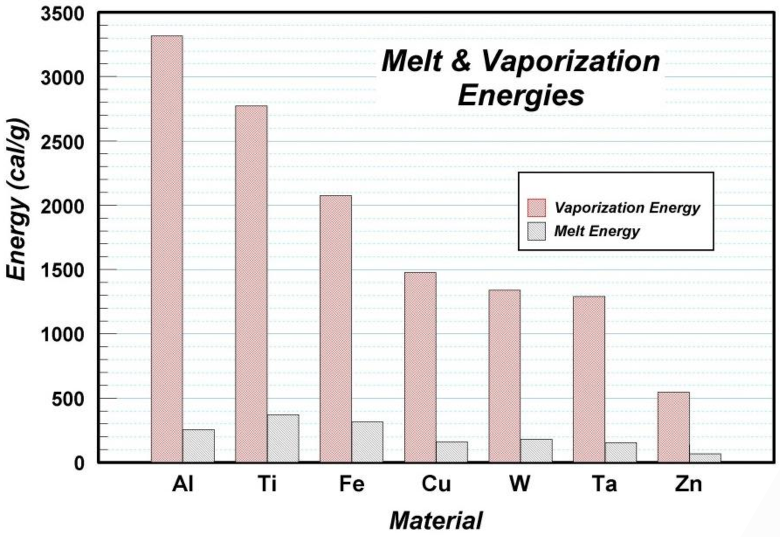

- Surrogate materials with lower vaporization energies effectively lower the velocity cliff.
- From the data at left, zinc is an ideal material for this purpose; its vaporization energy is almost 7 X lower than that for aluminum.

Velocities above the cliff can be achieved with:

- 3-stage launcher (velocities to ~16 km/s; w/ good diagnostics);
- Z machine (velocities to ~30 km/s, but expensive; w/ difficult diagnostics).

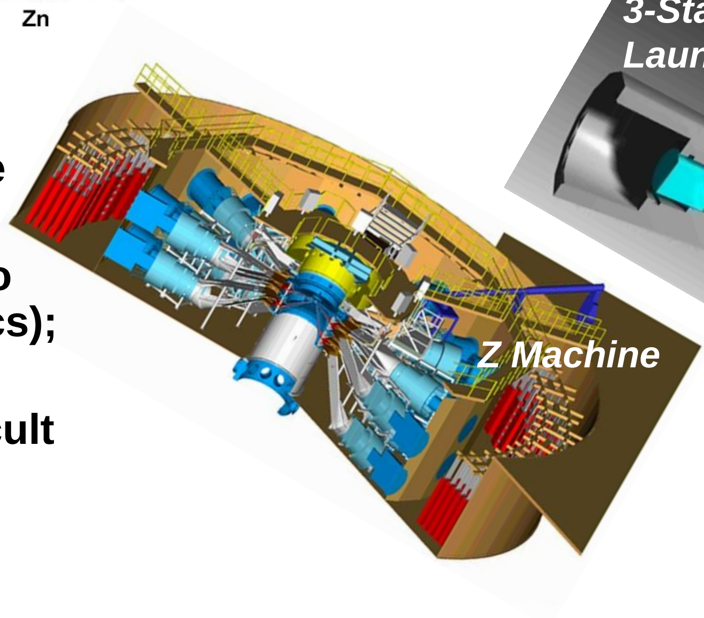

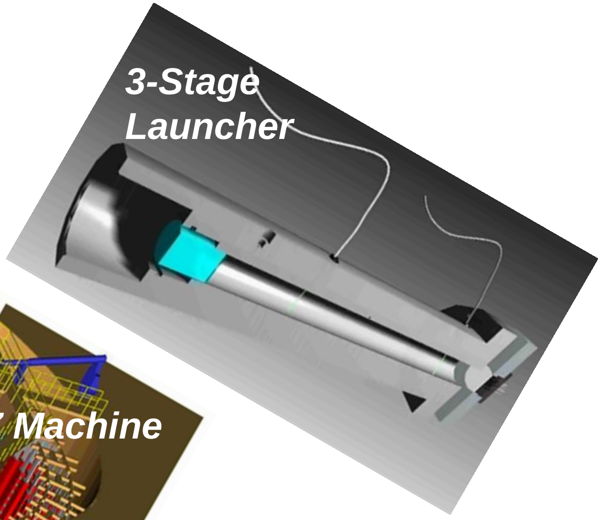

Sandia National Laboratories

Experimental investigations are usually centered on multi-stage light-gas guns.

Two-Stage Light-Gas Gun
(plates to ≤ 8 km/s)
Third stage can double velocity

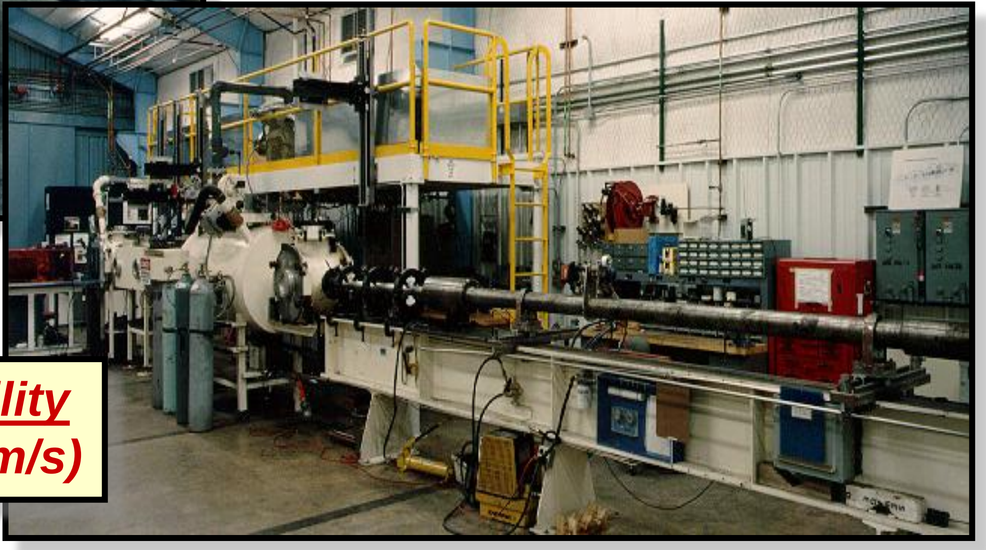

Terminal Ballistics Facility
(small spheres to ≤ 7 km/s)

Sandia National Laboratories

The projectile-shape dependence of debris clouds has been studied experimentally.

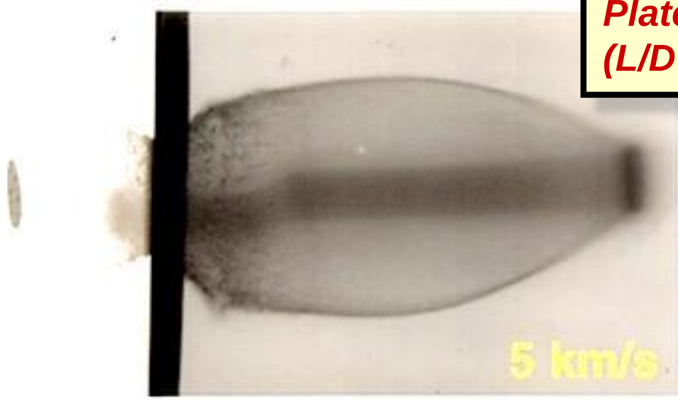

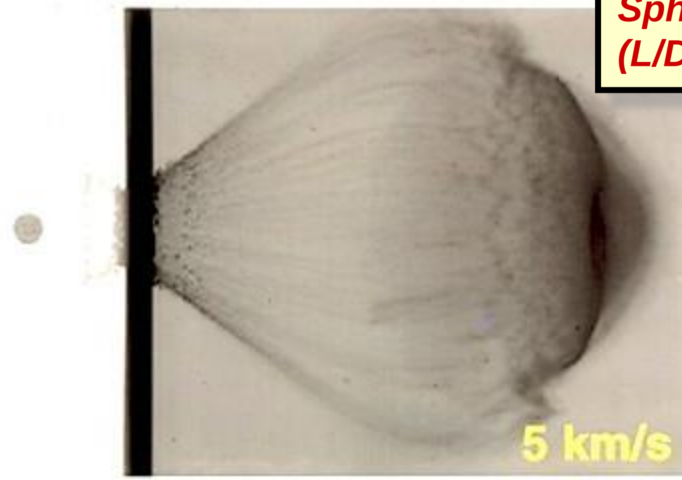

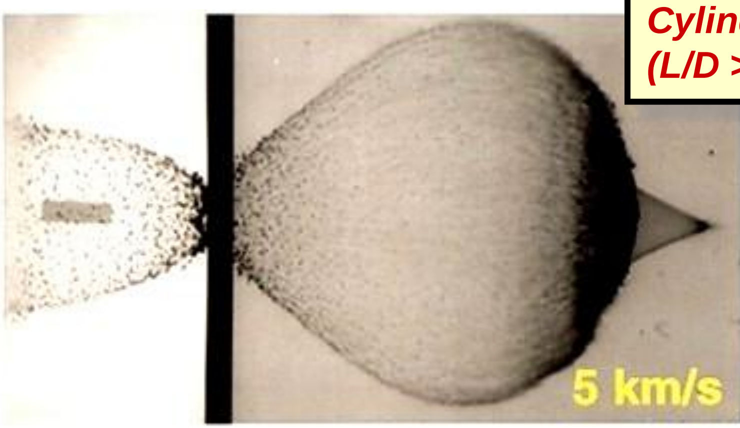

As projectiles transition from plate, to cylinder, to sphere, lateral debris-cloud velocities increase, but debris-front velocities remain constant.

Zinc projectiles on zinc targets—representative of "above-the-cliff" interactions via surrogate mat'ls

– Data adapted from Konrad (1994).

Sandia National Laboratories

There are different approaches for modeling impacts, but all must be validated with experiments.

- **Methods of analysis extend from simple scaling laws, to detailed analytic models, to elaborate multi-D hydrocode analyses. The latter provide point calculations, often on complex configurations, which can obscure trends. The former are often needed to clarify the overall behavior.**
- **Other phenomena that modeling can address include fragmentation and, for *hypervelocity* impacts, momentum enhancement.**
- **All modeling approaches and phenomena need to be validated with experiments, above and below the velocity cliff, as appropriate.**

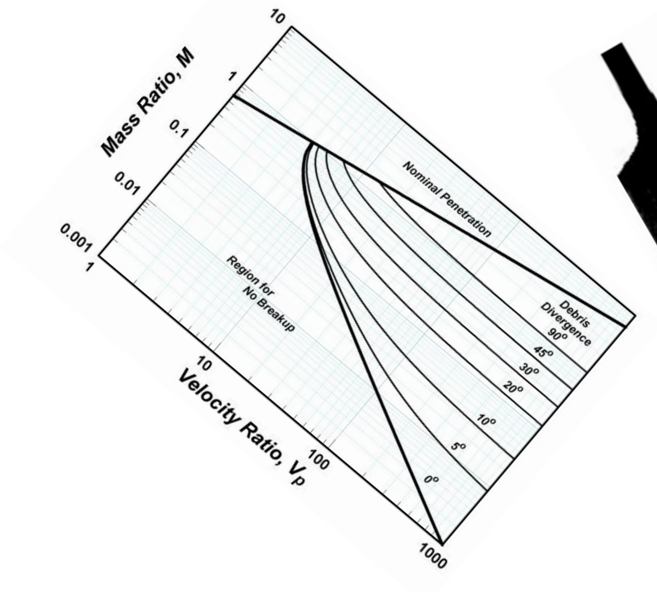

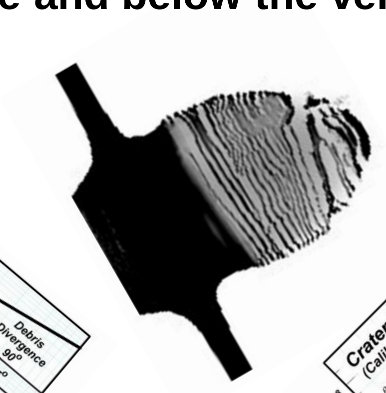

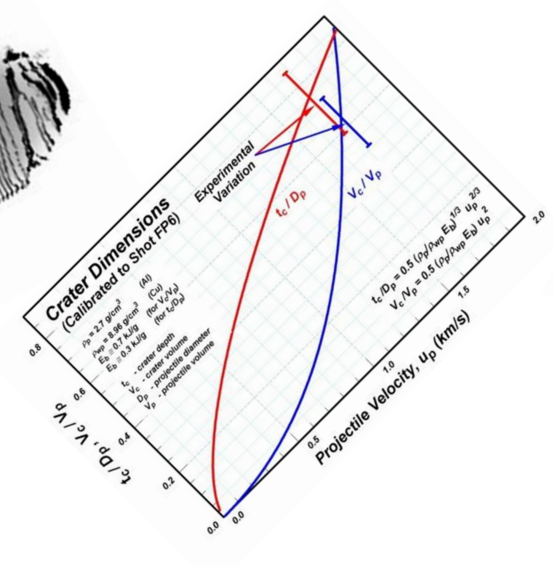

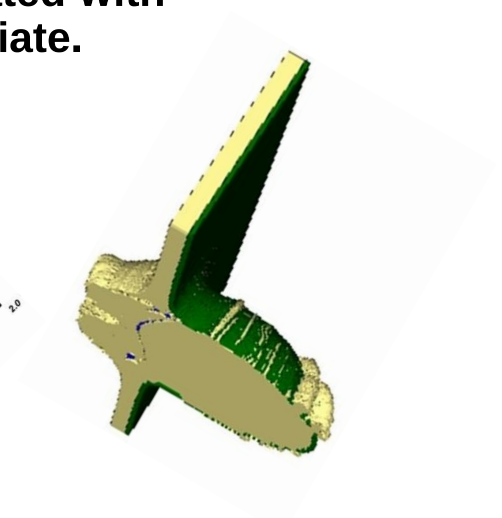

– See Grady (1995) & Lawrence (1990) for fragmentation & momentum enhancement.

Sandia National Laboratories

Debris behavior can be studied with analytic models developed for stand-off particle shields.

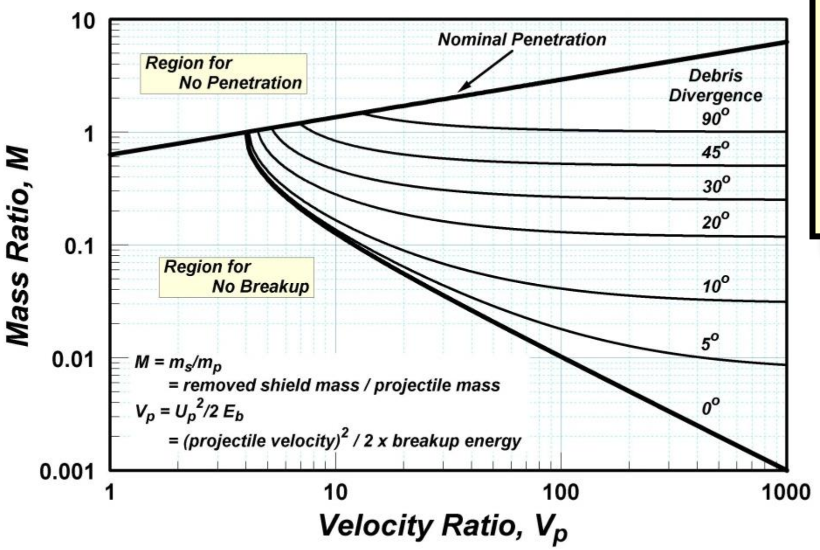

- ***This analytic model describes the expansion of debris clouds resulting from the impact of chunky projectiles on stand-off or Whipple bumper shields.***
- ***Stand-off shields can provide the most efficient protection for space-based assets.***

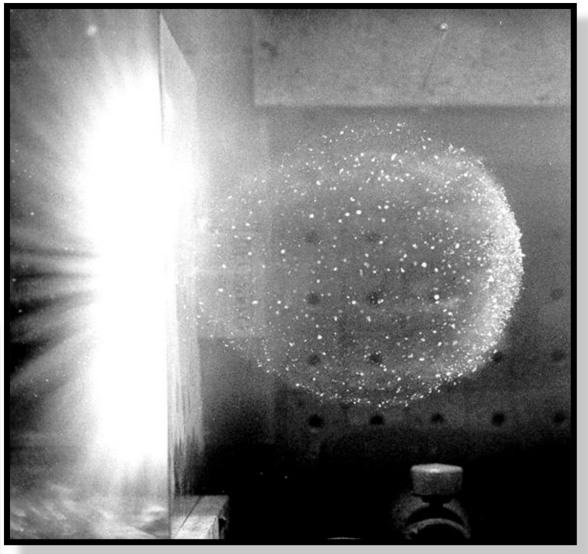

$M \approx 0.6$
$V_p \approx 7.5$
$\theta \approx 30°$
*$E_b \approx 1.2$ kJ/g **

** $E_b = 0.9\,E_m$ for steel*

- ***This debris cloud was generated by the impact of a 6.3-mm steel sphere on a 0.63-mm steel sheet at 4.22 km/s.***
- ***The impact velocity is below the velocity cliff and the debris consists mostly of fragments.***

– Model & data from Lawrence (1992a) & Ang (1993).

Sandia National Laboratories

Enhanced momentum transfer occurs when hyper-velocity particles impact thick targets.

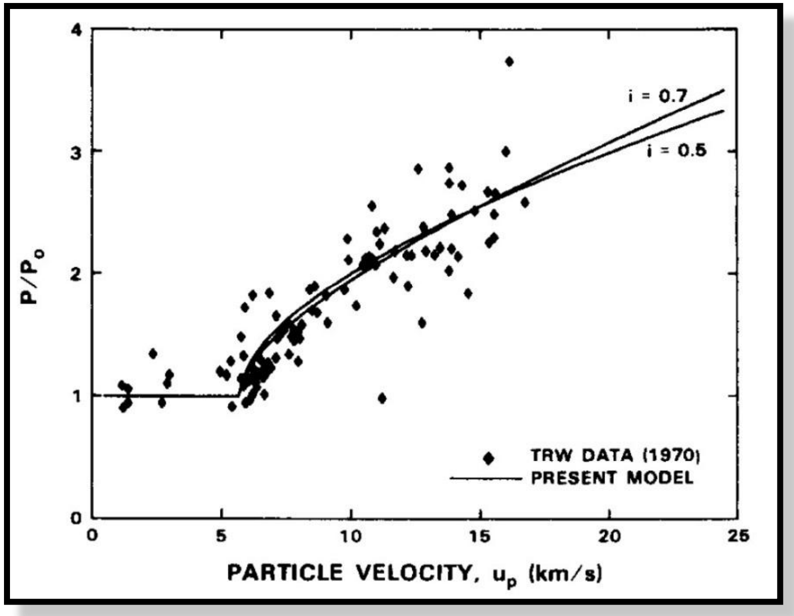

- *These NASA data are from TRW, taken by Slattery and Roy (1970), and represent the impact of submicron-size iron particles on a 5-µm-thick stainless steel membrane.*
- *The data show a great deal of scatter, but the trend is evident, with enhancement factors (P/P_0) approaching 3 X at a velocity of ~15 km/s.*

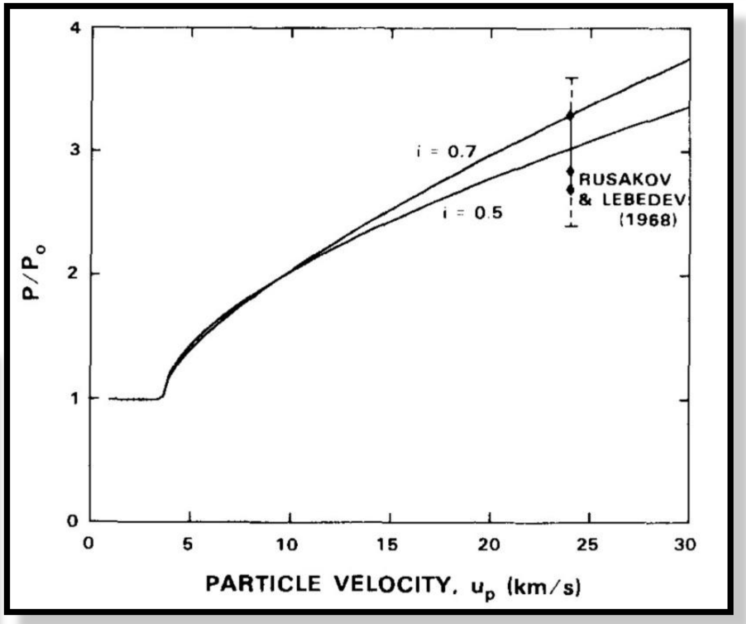

- *Russian data, from Rusakov and Lebedev (1968), although more sparse, are for tungsten particles impacting steel targets.*
- *The model calculations in both plots are similar, with parameter adjustments for the different projectile materials.*

– Momentum enhancement model from Lawrence (1990).

Sandia National Laboratories

Experimental and numerical debris-cloud radiographs confirm hydrocode validation . . .

Shot SHV-2 (~12 μs):

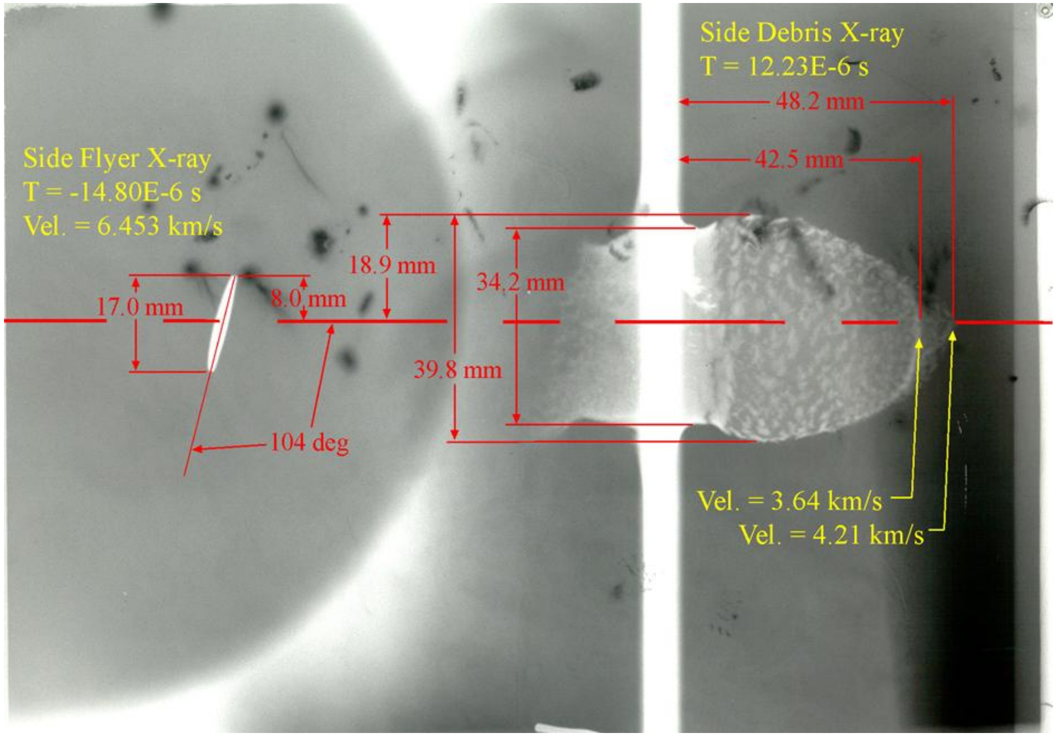

CTH / SHV-2 (~12 μs):

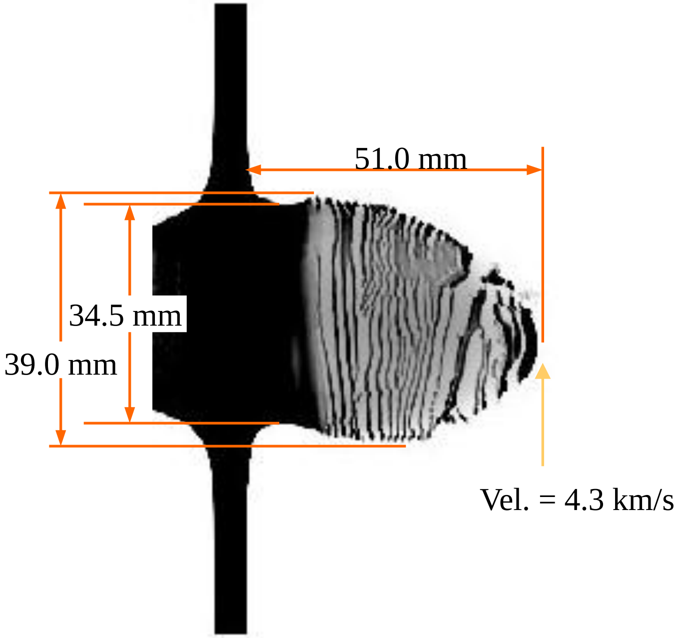

Flyer impact was at 6.49 km/s, with a tilt angle of ~20°. The target was an aluminum-backed ablator.

. . . however, the fragmentation of the aluminum backing, which provides an "envelope" around the debris cloud, shows qualitative differences.

Sandia National Laboratories

Gas-gun impacts at 6.5 km/s can be simulated well for an aluminum target . . .

***Shot CLP-2* (14.3 μs):**

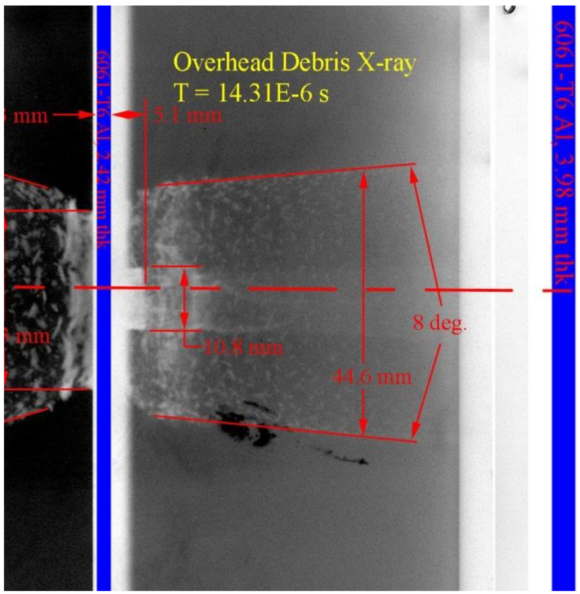

***CTH / CLP-2* (14.0 μs):**

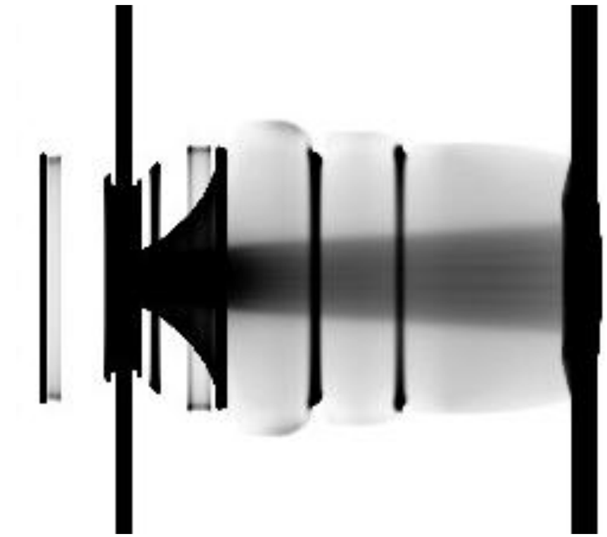

Flyer R_{curv} = 65.2 mm

Debris-cloud shape — slightly diverging
Debris-cloud diameter = 41.7 – 44.6 mm
Core diameter = 10.8 – 12.8 mm

Debris-cloud shape — mostly columnar
Debris-cloud diameter = 43.5 mm
Core diameter = 10.1 – 15 mm

. . . however, calculated debris-cloud failure patterns are influenced by numerical algorithms.

Sandia National Laboratories

The response of long-rod ($L/D >> 1$) penetrators is also simulated well with hydrocodes.

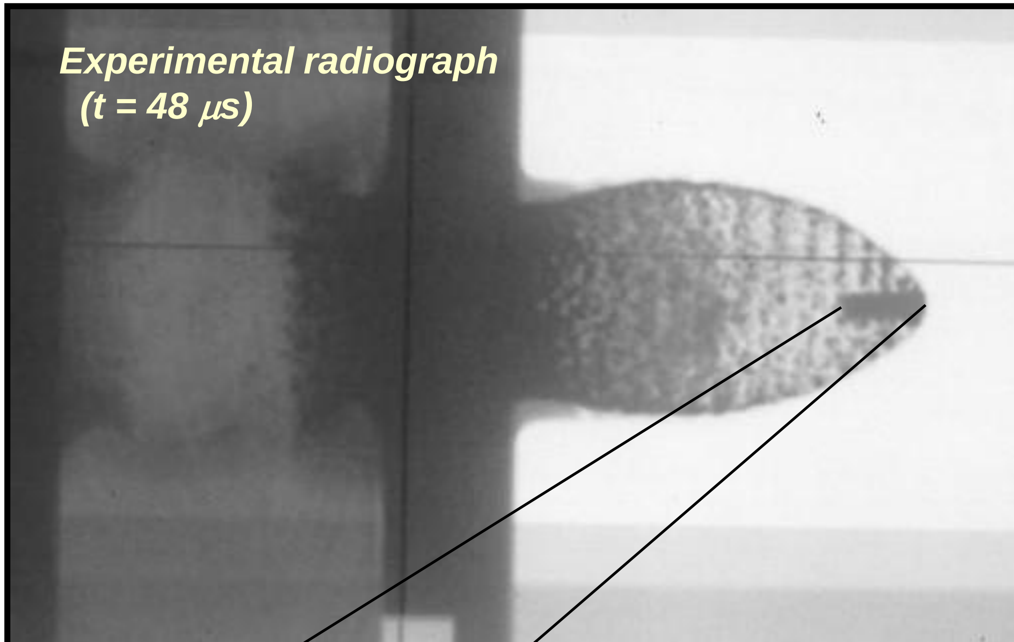

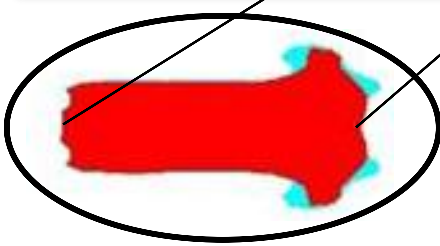

2-D CALE
(t = 48 μs)

Experimental measurement and 2-D CALE calculation of a 58-mm long tungsten rod after penetrating multiple spaced target layers agree well. The eroded rod lengths are both ~14 mm. The initial impact velocity was 4.8 km/s.

Impacts on similar oblique targets (here at 45°) show good penetration, and agreement with measured eroded rod length. However, the rod shows some late-time rotation due to the interaction.

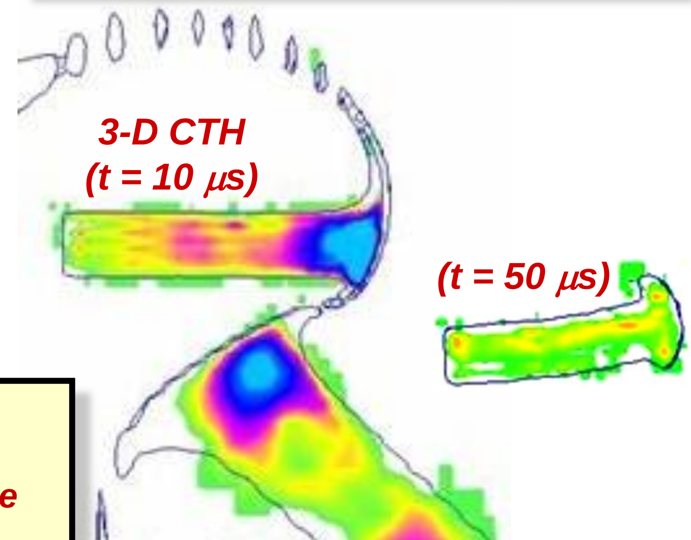

$V_0 = 4.5$ km/s

– Data & calculations adapted from Vetrovec (2001).

Sandia National Laboratories

Even craters generated by flat plates can be correlated with relatively simple scaling laws.

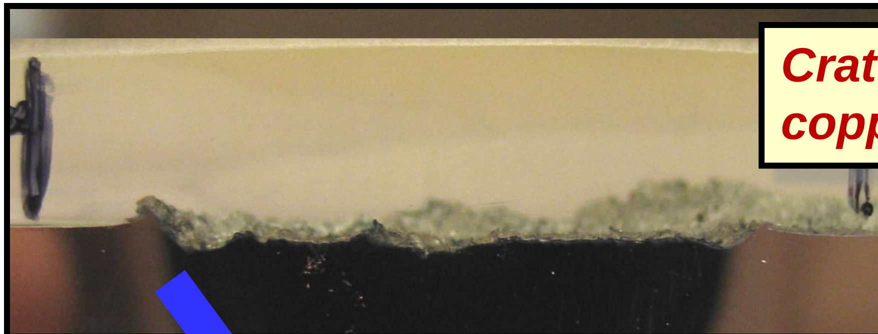

Crater cross-section from copper witness plate

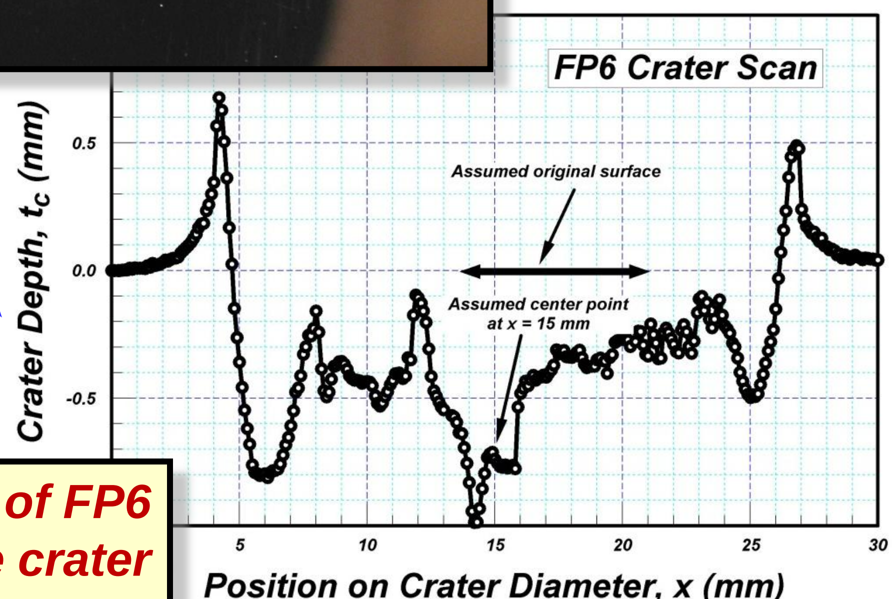

Numerical scan of FP6 witness-plate crater

D_p = ~0.6 mm
V_p = ~230 mm^3
u_p = ~2 km/s
t_c = 0.43 ± 0.08 mm
V_c = 142 ± 25 mm^3

D_p – projectile diameter
V_p – projectile volume
u_p – projectile velocity
t_c – crater depth
V_c – crater volume

– ~2 km/s aluminum flyer impacting a copper witness plate (shot FP6 from WSU).

Sandia National Laboratories

Scaling laws using “melt” energies correlate crater depth and volume with projectile parameters.

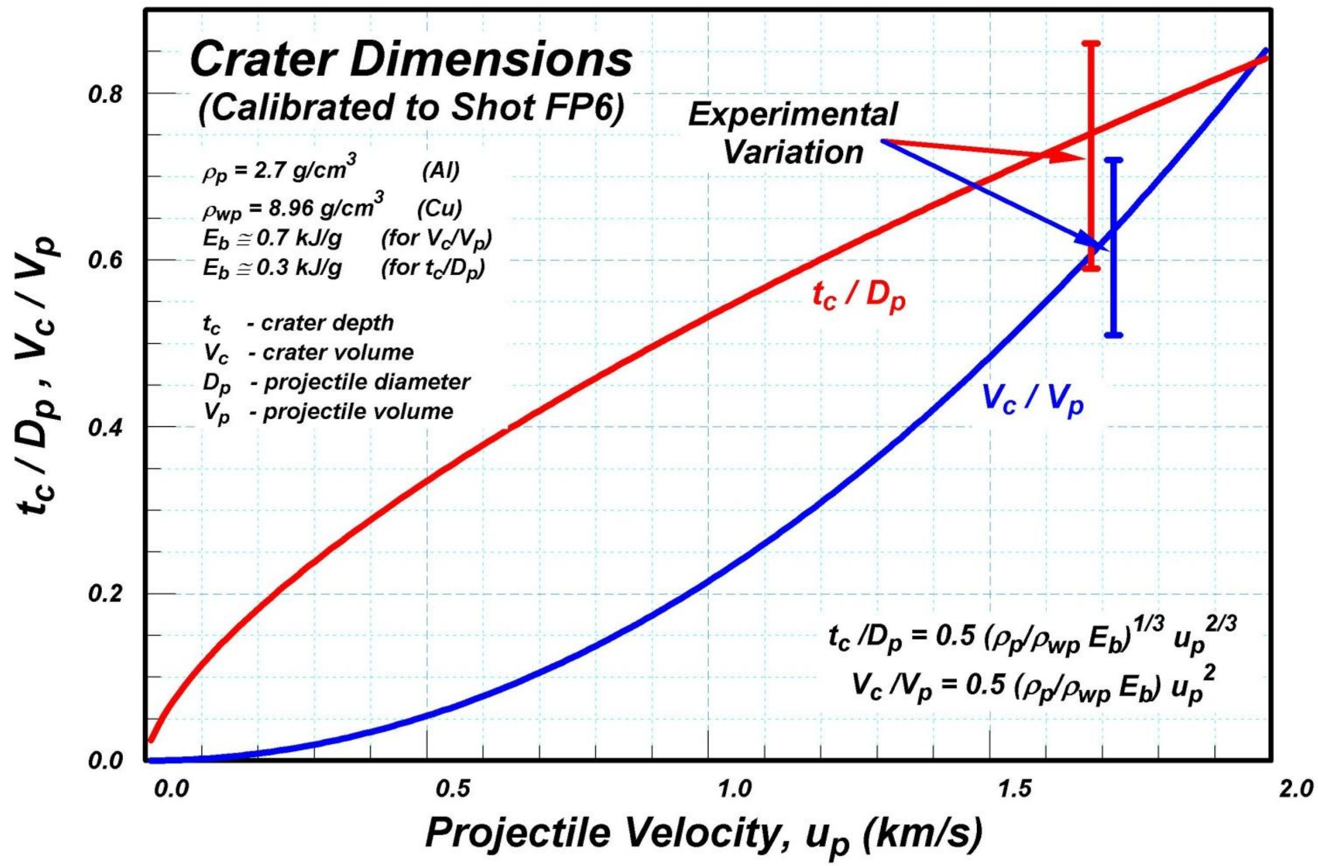

– Crater depth & volume scaling based on Anderson (1992) & Lawrence (1990).

Sandia National Laboratories

Analytic impulse models may be the simplest tools for initial NEO mitigation studies.

- **One recent application is Near Earth Object (NEO) mitigation:**
  - > **The impact on Earth by an NEO such as a large asteroid or comet could have catastrophic consequences. Altering its trajectory at a time and location early enough to preclude such a collision is probably the first line of defense.**
  - > **NEO mitigation technologies that have been proposed include: tractoring; magnetic deflection; and attacks with nuclear explosives. The latter involve direct comminution or breakup, and dynamic radiation loading by either neutrons or X rays generated by stand-off detonations.**
  - > **Because a generic nuclear explosive releases ~3/4 of its total energy as low-energy X rays, this last approach is probably the most promising one for study.**
- **There are many—but solvable—issues with this mitigation technology:**
  - > **The radiation / momentum-generation interaction phenomenology and its non-linearities must be well understood.**
  - > **The NEO engagement geometry must be analyzed, and the launch and transport requirements must be determined; they incorporate the needed trajectory deflection coupled with the timing of the engagement.**
  - > **Design and sizing of requisite nuclear devices, incorporating spectral optimization and total output, must be accomplished.**
- **However, the overall technology *IS* achievable with currently available capabilities and expertise.**

– See Hammerling (1995) for an early analysis.

Sandia National Laboratories

For parameter studies and scoping analyses, these models are probably the ideal tools.

- **There are two complementary approaches for addressing these problems:**
  - > 1-D and multi-D hydrocode calculations; and
  - > Simple closed-form analytic models.
- **Hydrocodes provide detailed time-dependent solutions for the dynamic interactions of interest.**
  - > These large codes often require extensive setup involving material equations of state and constitutive models, geometric target descriptions, and various source terms such as initial and boundary conditions.
  - > Because of their complexity, these codes are expensive to run, both in terms of time and effort. The number of cases examined can thus be severely limited.
- **The analytic models were originally developed in the 1960s and 1970s to investigate nuclear weapon effects.**
  - > Impulse-driven structural response was one of the most important modes of target response and vulnerability. Hence analytic models based fundamentally on conservation of energy and momentum were developed to calculate the impulse generated by high-intensity pulsed radiation loads. Historically they have been called the BBAY and MBBAY models.
  - > The important advantage of these models is that they are fast running and easy to set up. In fact, they often require only one input parameter with any significant degree of uncertainty (the target decomposition energy, E_0). Many cases can thus be studied without difficulty.

The MBBAY model uses conservation laws to predict the impulse from dynamic radiation loads.

- **The basic MBBAY model can be expressed as:**

$$I = \alpha\sqrt{2}\left[\int_0^{z_0}\left\{E(z) - E_0\left(1 + \ln\frac{E(z)}{E_0}\right)\right\}\rho^2\, z\, dz\right]^{1/2}$$

  > **Where** I **is the impulse,** $E(z)$ **is the deposited energy as a function of target depth** z**,** E_0 **is the material decomposition energy,** $E(z_0) = E_0$**,** ρ **is the target density, and** $1 \le \alpha \le 2^{1/2}$**.**

  > **This expression may need to be numerically integrated over the appropriate photon energies to account for major variations in material absorption coefficients.**

- **If the target material can be assumed to have a single "effective" absorption coefficient,** μ_{eff}**, then the above expression yields a closed-form solution:**

$$I^* = \alpha\sqrt{2}\left\{\Phi_0^* - \left[1 + \ln\Phi_0^* + \frac{1}{2}(\ln\Phi_0^*)^2 + \frac{1}{6}(\ln\Phi_0^*)^3\right]\right\}^{1/2}$$

  > **Where the variables have been given in non-dimensional form, *i.e.*,** $I^* = \mu_{eff}\, I / E_0^{1/2}$ **for the impulse, and** $\Phi_0^* = \mu_{eff}\, \Phi_0 / E_0$ **for the on-target energy fluence.**

  > **At high fluences, this solution takes on very simple square-root scalings for impulse,** $I^* = \alpha\,(2\,\Phi_0^*)^{1/2}$**, and for coupling efficiency,** $C_M^* = \alpha\,(2/\Phi_0^*)^{1/2}$**, both for** $\Phi_0^* >> 1$**.**

– For model description see Newlander (1978) & Lawrence (1992b).

Sandia National Laboratories

The MBBAY model leads to several very simple relationships for the key parameters.

- **Key parameters include the following:**
  - > **For the threshold fluence for impulse generation,** $\Phi_0^{*} = 1$**;**
  - > **For the fluence yielding the peak coupling coefficient** $(C_M)_{max}$, $\Phi_0^{*} \approx 10$**; and**
  - > **To reiterate, the high-fluence scaling leads to** $I^{*} = \alpha\,(2\,\Phi_0^{*})^{1/2}$, **and** $C_M^{*} = \alpha\,(2/\Phi_0^{*})^{1/2}$**, both for** $\Phi_0^{*} >> 1$**.**
  - > **Note that in the latter, high-fluence regime, the conversion efficiency is lower, but there is little uncertainty in the overall coupling level, including with respect to** E_0**. This also provides a clear indication how source design might be altered to control these parameters.**

Impulse:

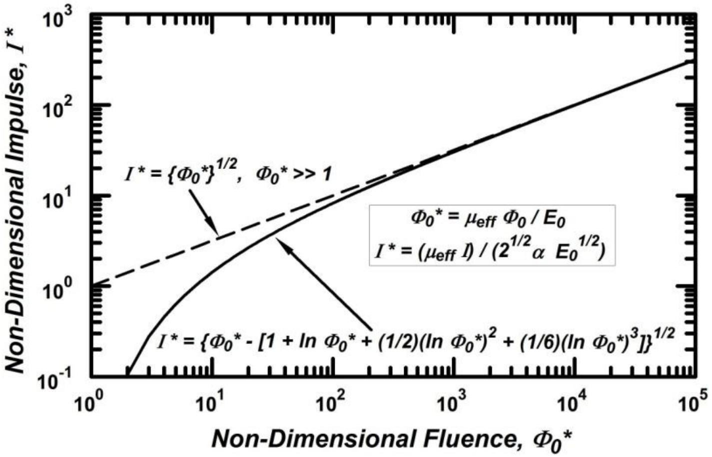

Coupling Coefficient:

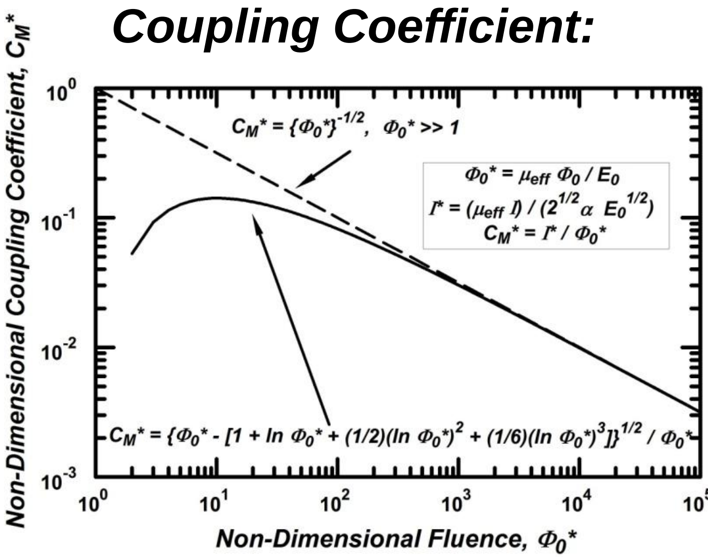

Sandia National Laboratories

The analytic models lead to requirements that, among others, should address validation.

- **As with any theoretical or computational study, V & V (verification and validation) are important issues.**
  - **Verification (*i.e.*, that the numerical techniques correctly solve the originally posed problem) will be left to others and not be addressed here.**
  - **We accomplish validation through comparison of model predictions with experimental results, primarily obtained through momentum or impulse measurements from relevant targets exposed to pulsed radiation loads in the Sandia Z-pinch machine.**
- **Z provided experimental conditions, relevant to operational scenarios, for NEO mitigation.**
  - **The radiation environment can be characterized as low-energy thermal (~0.2 keV blackbody) superimposed with small characteristic wire-array line spectra. Appropriate X-ray fluences of ~1 kJ/cm^2 were available.**
  - **Samples of representative NEO materials, with their properties, were used for testing.**
- **For actual parametric variations to establish feasibility for possible operational scenarios, spectra and fluences need to be established.**
  - **Simple variations of X-ray spectra (*i.e.*, using Planckian temperatures) represent well the operationally achievable loading environments.**
  - **To understand the nonlinear radiation/impulse coupling, we must examine fluence regimes to establish threshold levels, to indicate peak coupling efficiencies, to show the limits for simple linear scaling, and to clarify how source design might help control these interaction phenomena.**

The Z machine provides a 200-eV thermal X-ray spectrum along with a smaller line output.

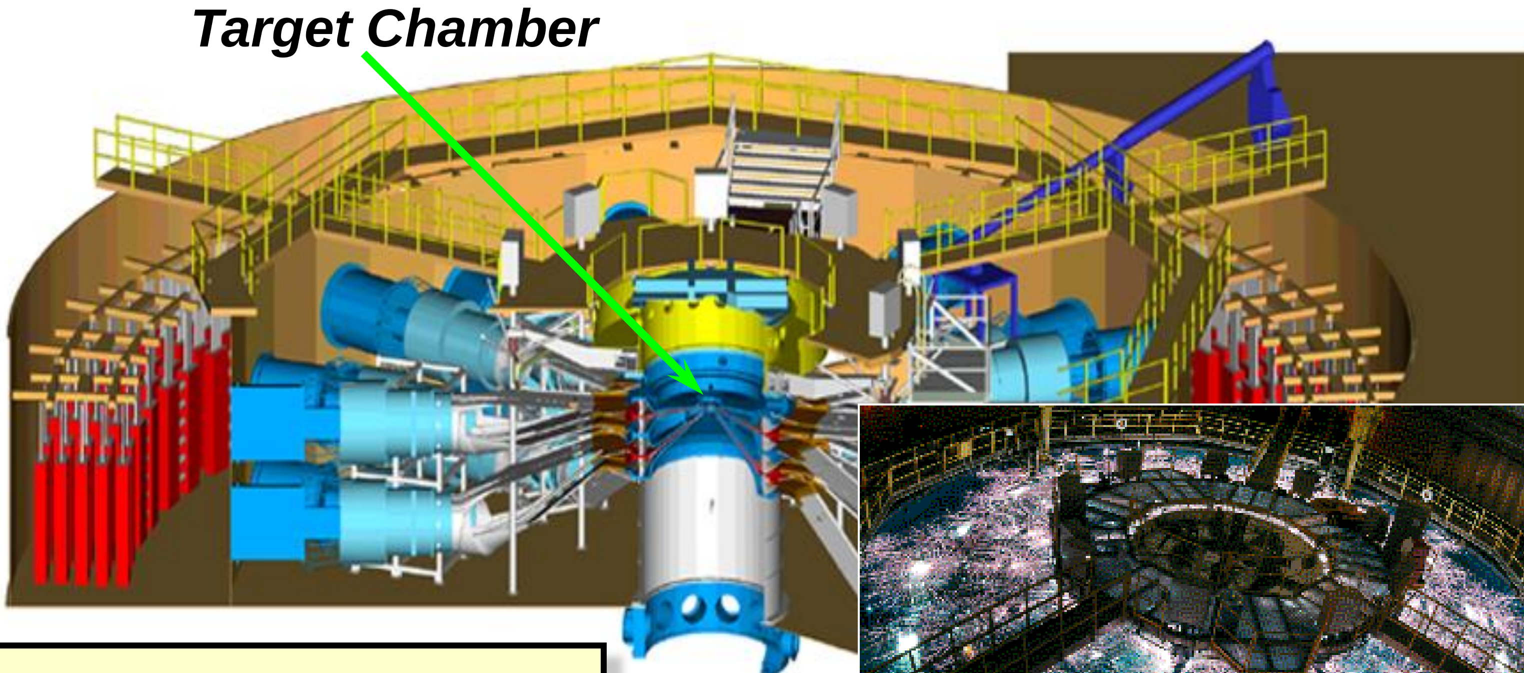

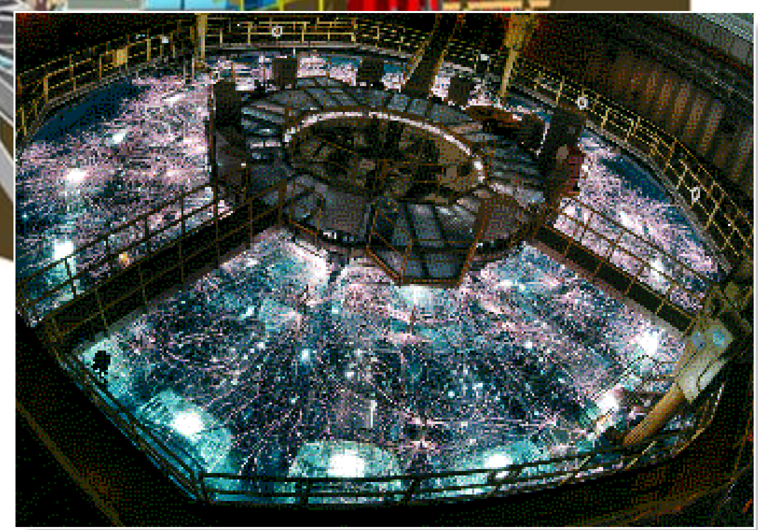

Z machine parameters:

- ***11.5 MJ stored energy***
- ***~22 MA peak current***

On-target parameters:

- ***~1 kJ/cm^2 energy fluence***
- ***~5 ns pulse width***

Sandia National Laboratories

Although differing from potential operational environments, the Z spectrum is qualitatively similar.

The major portion of the Z spectrum consists of a 200-eV thermal blackbody superimposed on a line spectrum characteristic of the imploding wire array (here copper). In this case the wire-array contribution is a small fraction of the total. In this plot the units are normalized to a total fluence of one.

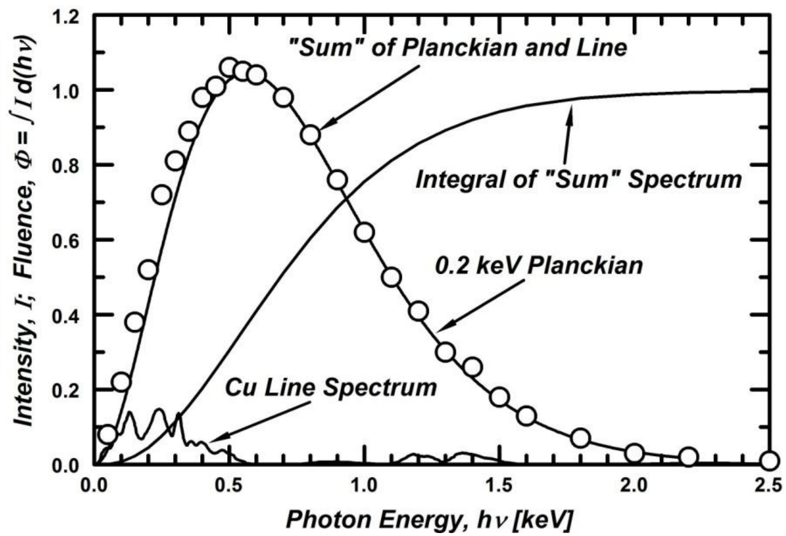

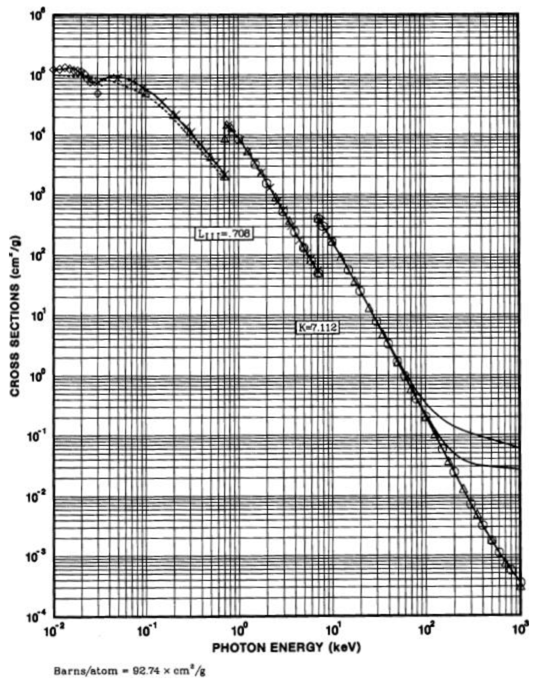

Typical energy absorption coefficients vary approximately with $(h\nu)^{-3}$, and have photoelectric absorption edges that reduce the value by nearly an order of magnitude at the various photon energies characteristic of the element (here iron). This extreme variation occurs over the photon energy regime being considered in this study, and thus must be appropriately incorporated.

Sandia National Laboratories

The Z validation experiments show a significant variation in agreement with the model.

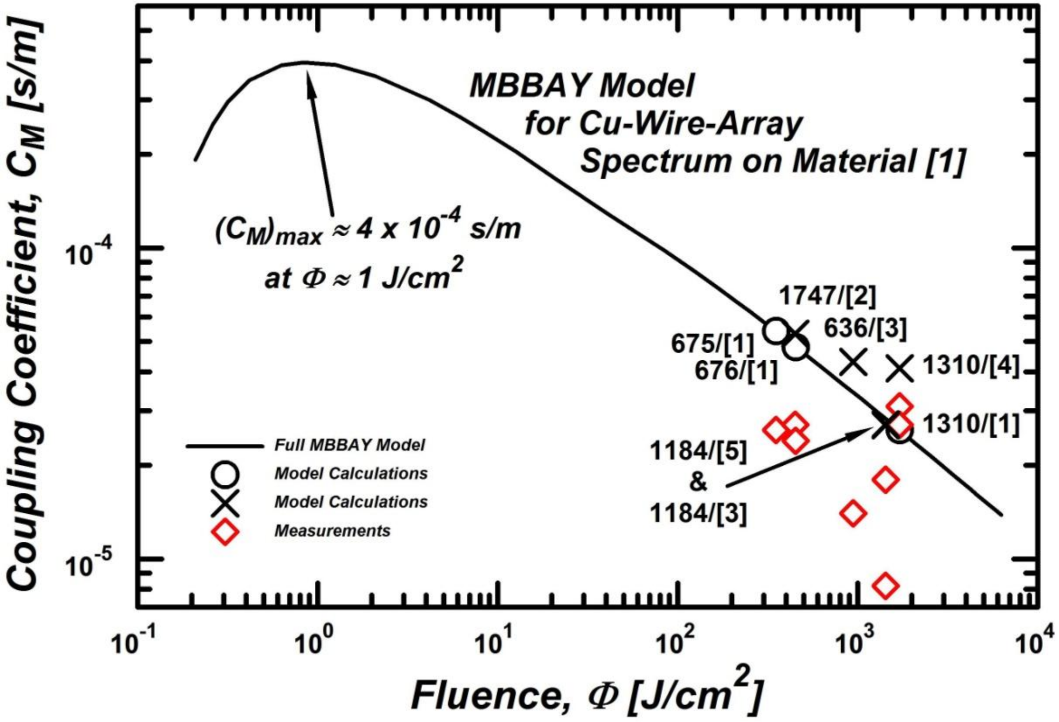

- ***The materials used for the Z experiments were:***
  - ***> [1] Allende***
  - ***> [2] Dunite***
  - ***> [3] Odessa***
  - ***> [4] Aluminum***
  - ***> [5] Iron***
- ***Values accepted by the community were used for E_0; however, they may be inappropriate for dynamic impulse coupling.***
- ***The MBBAY model calculations used Allende with the Cu-wire-array X-ray spectrum.***
- ***Although varied, the agreement of the data with the model points the way for system-level system studies.***

– For descriptions of this work see Remo (2011) & Lawrence (2011).

Sandia National Laboratories

A **parameter study** using potential operational conditions shows useful results and trends.

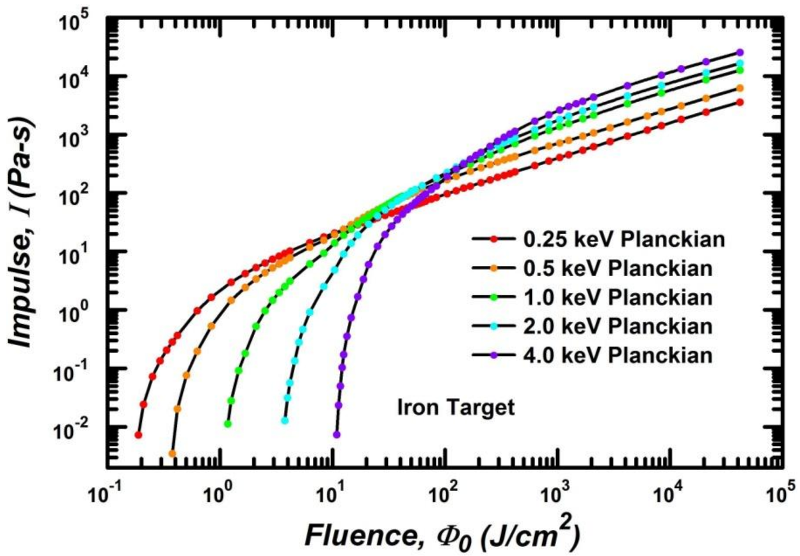

- *These model calculations used iron targets (a common constituent material for NEOs), and blackbody X-ray spectra varying from 0.25 keV to 4 keV.*
- *Fluences varied from as low as 0.1 J/cm^2 (to capture the impulse thresholds) to 10^5 J/cm^2 (to illustrate high-fluence limits).*

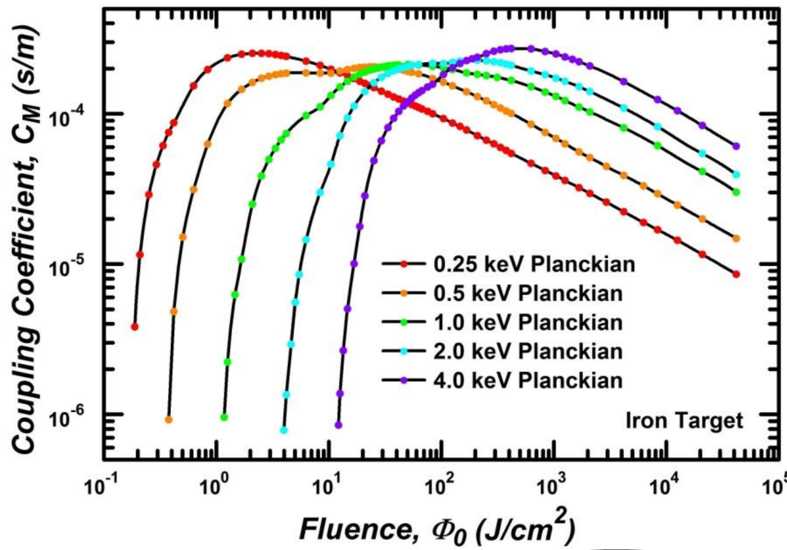

- *Impulse, I, and impulse coupling efficiencies, C_M, are shown, both as functions of X-ray fluence.*
- *Nonlinearities, represented by impulse thresholds and peak coupling coefficients, are evident. Slight irregularities in the curves are due to the discontinuities in the iron absorption coefficients.*

– For code description see Lowen (1993).

Sandia National Laboratories

Using analytic impulse models to study NEO mitigation has led to several useful conclusions.

- Direct use of nuclear devices for NEO deflection is feasible with today's technology.
  - With adequate warning a catastrophic impact could be avoided by appropriate course deflections.
  - In contrast to other proposed techniques, pulsed X rays generated by nuclear devices provide probably the most efficient approach.
  - No new technological advances are required.
- Simple analytic models are ideal for system-level parameter studies for relevant pulsed-radiation-generated impulse phenomena.
  - The models have only one possibly uncertain parameter (E_0), and are thus easily calibrated with limited reference data.
  - The models yield simple forms for impulse thresholds, peak coupling coefficients, and high-fluence scaling relationships.
  - Although the models are simple, they clarify the nonlinear interaction phenomena involved, and yield data for optimized source design.
  - Additional but limited full-scale hydrocode calculations could/should be used to expand on the results of the analytic-model parameter studies.
- Although not examined here, NEO engagement studies—for both timing, and for interaction and loading geometries—can be achieved relatively easily once the impulse coupling relations are established.

Selected references . . .

- C. E. Anderson Jr. *et al*., *A Penetration Mechanics Database*, SwRI Report 3593/001, Southwest Research Institute, San Antonio, TX (1992).
- J. A. Ang *et al*., "Pulsed Holography for Hypervelocity Impact Diagnostics," *International Journal of Impact Engineering*, V. 14, p. 13 (1993).
- D. E. Grady & M. E. Kipp, "Experimental Measurement of Dynamic Failure and Fragmentation Properties of Metals," *International Journal of Solids and Structures*, V. 32, No. 17/18 (1995).
- P. Hammerling & J. L. Remo, "NEO Interaction With Nuclear Radiation," *Acta Astronautica*, V. 36, p. 337 (1995).
- C. H. Konrad *et al*., "Dependence of Debris Cloud Formation on Projectile Shape," *High Pressure Science and Technology—1993*, S. C. Schmidt *et al*., Eds., American Institute of Physics, New York (1994).
- R. J. Lawrence, "Enhanced Momentum Transfer from Hypervelocity Particle Impacts," *International Journal of Impact Engineering*, V. 10, p. 337 (1990).
- R. J. Lawrence, "A Simple Approach for the Design and Optimization of Stand-Off Hypervelocity Particle Shields," Paper No. AIAA 92-1465, AIAA Space Programs and Technologies Conference, Huntsville, AL (1992a).
- R. J. Lawrence, "The Equivalence of Simple Models for Radiation-Induced Impulse," *Shock Compression of Condensed Matter—1991*, S. C. Schmidt *et al*., Eds., Elsevier Science Publishers, Amsterdam (1992b).
- R. Lowen *et al*., *XRAY Radiation Transport Program (User's Handbook)*, Horizons Technology, Inc., San Diego, CA, DNA-EH92-012-G-V1 (HTI-SDR-92-051), Defense Nuclear Agency, Alexandria, VA (1993).
- C. D. Newlander *et al*., *Nuclear Hardness Evaluation Procedures (NHEP) Program, Phase 1: Analytic Technique Survey*, AFWL-TR-78-18, Air Force Weapons Laboratory, Kirtland AFB, NM (1978).
- M. M. Rusakov & M. A. Lebedev, "Determination of Recoil Momentum Owing to Meteoritic Impact in a Simulation," Translated from *Kosmicheskie Issledovaniya*, V. 6, No. 4, p. 634 (1968).
- J. C. Slattery & N. L. Roy, *Investigation of Hypervelocity Microparticles Impact Phenomena*, NASA CR-66872, TRW System Group, Redondo Beach, CA (1970).
- J. Vetrovec *et al*., "Analysis and Testing of Rod-Like Penetrators in the 4–5 km/s Regime," *International Journal of Impact Engineering*, V. 26, p. 797 (2001).

Sandia National Laboratories

. . . and two in the queue.

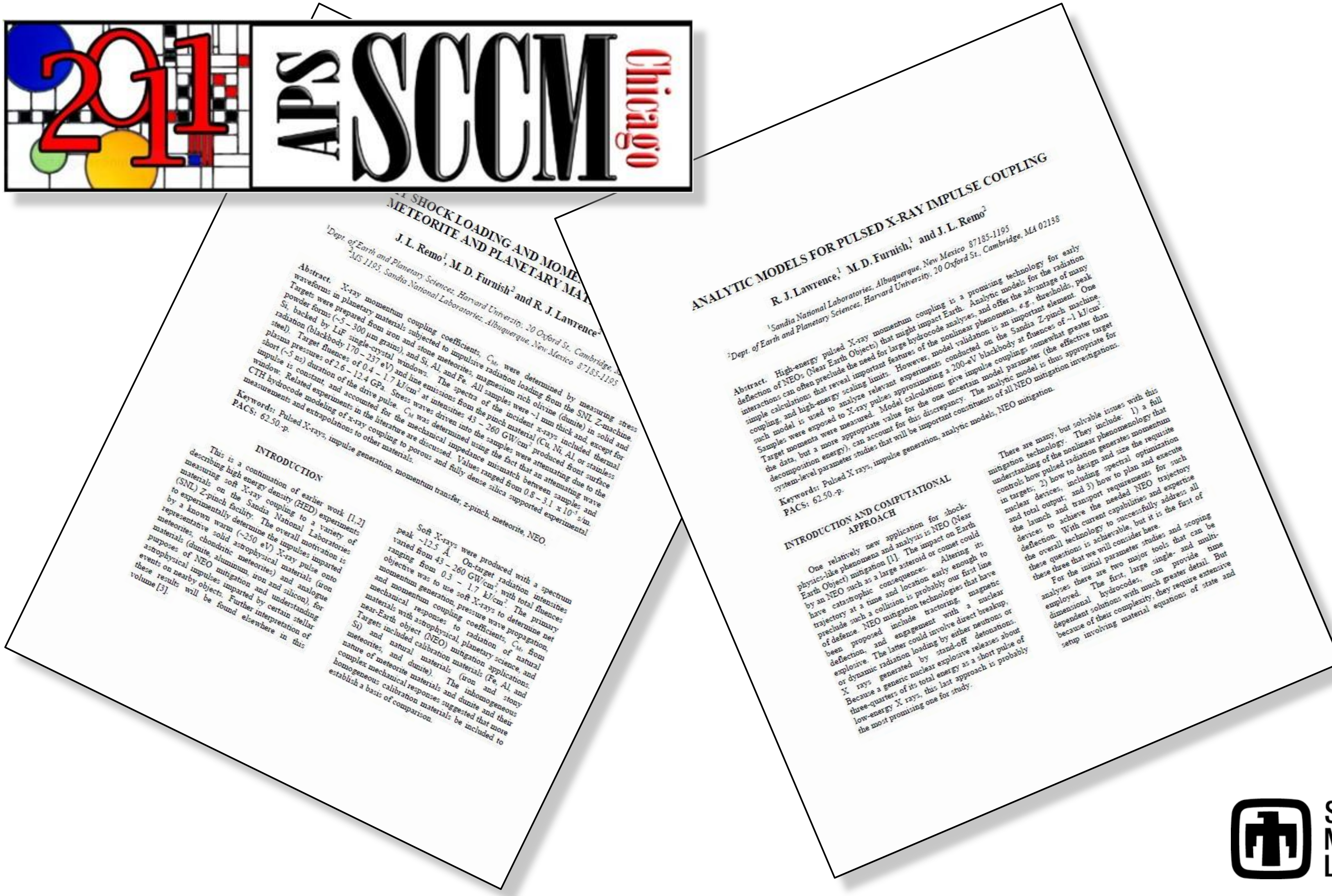

Sandia National Laboratories